Investigations of The Origin of Phase Differences Seen with Ultrashort TE Imaging of Short T2 Meniscal Tissue

M. Carl[1]
[1]Global Applied Science Laboratory, GE Healthcare, San Diego, CA, United States

Introduction: Ultrashort echo time (UTE) MRI utilizes specialized pulse sequences with nominal TEs as low as several microseconds to acquire signals from the short T_2 tissues frequently encountered in the musculoskeletal system [1]. Magnitude images are usually reconstructed and often show relatively low tissue contrast. We were surprised to see phase images of the meniscus obtained with these sequences showing remarkably high contrast in spite of the very short nominal TE of UTE sequences. We have used the Bloch equations, simulations, phantom experiments, and tissue studies to investigate the origin of this contrast.

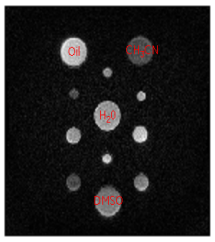

Fig.1: Magnitude and phase image of phantom setup containing different chemical components

Theory: With a standard gradient recalled echo (GRE) sequence TE is a well defined quantity, starting at the center of the RF pulse and ending at the center of the data acquisition (DAQ) window where k = 0. The phase evolution during a GRE sequence (Φ_{TE}) of a spin with off-resonance frequency $\omega_{off} = 2\pi f_{off}$ is given by: $\Phi_{TE} = \omega_{off} TE$

In comparison, in a typical 2D UTE sequence the nominal TE is defined as the time from the end of the RF pulse to the beginning of the data acquisition (k = 0). Using the phase expression above, with a nominal TE of 12 µs for example, little or no phase evolution or phase contrast would be expected. However, with a UTE sequence the nominal TE does not include the phase evolution during excitation or readout. The overall phase in the final MR image therefore contains contributions from three periods, namely that of the RF pulse, TE, and the duration of the data acquisition so that:

$$\Phi = \Phi_{RF} + \Phi_{TE} + \Phi_{DAQ} = \Phi_{RF} + \omega_{off} \cdot TE + \Phi_{DAQ}$$

Phase Evolution During the RF Pulse: The differential equation for the complex magnetization $M = M_x + iM_y$ during an arbitrary RF pulse $B_1(t)$ of duration τ and slice selection gradient $G_s(t)$ in the small tip angle approximation is given by: $dM/dt + i\,\omega_z M = i\,\gamma B_1 M$ [2], where in our case $\omega_z = \gamma G_s z - \omega_{off}$. With 2D UTE sequences slice-selective excitation is repeated twice (in separate TRs), with the slice selection gradient reversed ($G_s \rightarrow -G_s$), and the complex data obtained after the excitations are added to generate the final slice profile:

$$M(\tau,z) = \frac{\gamma M_0}{2}\left(e^{-i\int_0^{\tau}(\gamma G_s(t)z-\omega_{off})dt} \int_0^{\tau} B_1(t) e^{i\int_0^{t}(\gamma G_s(t')z-\omega_{off})dt'} dt + e^{-i\int_0^{\tau}(-\gamma G_s(t)z-\omega_{off})dt} \int_0^{\tau} B_1(t) e^{i\int_0^{t}(-\gamma G_s(t')z-\omega_{off})dt'} dt \right)$$

Hence, the phase contribution from the RF pulse can be calculated using: $\Phi_{RF} = \angle\left\{\int_z M(\tau,z)dz\right\}$ [1]

Phase Evolution During the Data Acquisition: The k-space signal using 2D UTE with radial ramp sampling (with slew-rate *slew* and ramp time T_{ramp}) followed by flattop sampling (at read gradient strength G) of an object with spin density m(r) and off-resonance ω_{off} is given by:

$$S(\vec{k}) = \int_V m(\vec{r}) e^{-i2\pi\vec{r}\cdot\vec{k}} e^{i2\omega_{off}\sqrt{\frac{\pi|k|}{\gamma \cdot slew}}} d\vec{r} \quad ramp$$

$$S(\vec{k}) = \int_V m(\vec{r}) e^{-i2\pi\vec{r}\cdot\vec{k}} e^{i\frac{2\pi\omega_{off}}{\gamma G}|k|} d\vec{r} \quad flattop$$

The image from such a signal in k-space can be calculated by inverse 2D Fourier transforms. Two approximations need to be made in order to obtain a closed-form solution for the phase in the reconstructed image: **1)** We will assume that the spin density m(r) is an order one Bessel function with spatial extend of L, so that the k-space signal magnitude is approximately a 2D disk with cutoff radius $|k| = (2L)^{-1}$. **2)** The image and corresponding phase is evaluated in polar coordinates only at the center of object (x = y = 0). Despite these approximations, the closed form solutions of the reconstructed image are still rather complicated. Nonetheless, the phase angles can be determined analytically and are summarized in Table 1. Similar calculations can be performed for 1D and 3D radial sampling. The two columns shown in Table 1 depend on whether the maximum k-space extent $(2L)^{-1}$ of the signal in k-space is reached during the ramp portion (k_{ramp}) of the read gradient (left column) or after that, during the flattop portion (right column).

	$\frac{1}{2L} < k_{ramp}$	$\frac{1}{2L} > k_{ramp}$
1D	$\Phi_{DAQ} \approx \frac{4}{3}\omega_{off}\sqrt{\frac{\pi}{2\gamma L \cdot slew}}$	$\Phi_{DAQ} \approx \omega_{off}\left(\frac{\pi}{2\gamma GL} + \frac{T_{ramp}}{2}\right)$
2D	$\Phi_{DAQ} \approx \frac{8}{5}\omega_{off}\sqrt{\frac{\pi}{2\gamma L \cdot slew}}$	$\Phi_{DAQ} \approx \omega_{off}\left(\frac{2\pi}{3\gamma GL} + \frac{T_{ramp}}{2}\right)$
3D	$\Phi_{DAQ} \approx \frac{12}{7}\omega_{off}\sqrt{\frac{\pi}{2\gamma L \cdot slew}}$	$\Phi_{DAQ} \approx \omega_{off}\left(\frac{3\pi}{4\gamma GL} + \frac{T_{ramp}}{2}\right)$

Table 1: Phase accrued during radial ramp and flattop sampling for 1D, 2D, and 3D UTE sequences. The left column corresponds to pure ramp sampling, while the right column corresponds to ramp plus flattop sampling.

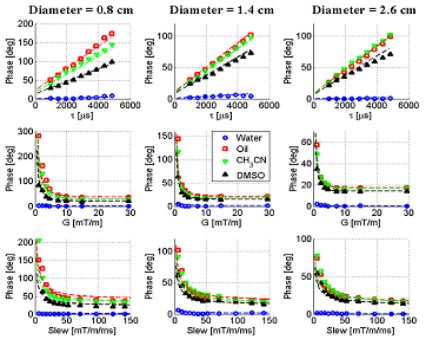

Fig.2: Experimental phases for the phantoms shown in Fig.1

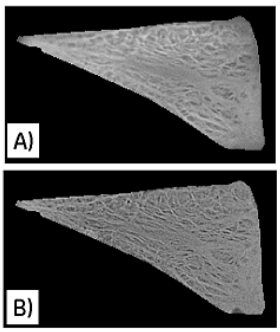

Fig.3: Meniscus specimen. A) Magnitude. B) Phase.

Method Experiments were conducted on phantoms and a meniscus specimen using a 3T clinical GE scanner. The phantom setup contained 12 cylindrical containers with three groups of sizes (diameters: 0.8 cm, 1.4 cm, and 2.6 cm) standing upright and imaged in a standard head coil. The four phantoms within each size group were filled with a different chemical species (Water, Oil, CH_3CN, and DMSO) to study the phase of the UTE images in the presence of different off-resonance frequencies. Next, a small meniscus sample was placed in a perfluorocarbon bromide (PFOB) filled syringe and imaged inside a custom built coil.

Results Fig.1 shows both magnitude and phase UTE images of the phantom. The experimental phases (measured in small ROIs placed around the center of the phantoms) imaged with various scanning parameters are shown in Fig.2. Superimposed as lines are the phases from the theoretical results from Eq.[1] and Table 1, and match the experimental phases well. Fig.3a shows a high-resolution 2D UTE magnitude image of the meniscus specimen at nominal TE = 12 µs. The corresponding phase image is shown in Fig.3b. This image exhibits higher contrast between the different fiber groups than the magnitude image. Using variable TE UTE images, the frequency difference between different fiber groups was found to be around 30-40Hz.

Conclusion UTE phase imaging is able to provide high contrast for short T_2 tissues. The phase images may show higher contrast and better defined boundaries of fiber structures than magnitude images. Significant phase evolution can arise at a field strength of 3T in the short TEs necessary to image short T_2 signals of the tissues. Major contributions to this phase evolution occur during RF excitation and data acquisition. In addition, previously unrecognized susceptibility differences between different fiber groups in the meniscus contribute to contrast in UTE phase images.

References: [1] M. D. Robson et. al, J. Comput Assist Tomogr 27, 6 (2003) [2] Nishimura, *Principles of Magnetic Resonance Imaging, Edition 1.1, 2010*